Contents lists available at ScienceDirect

Journal of Natural Gas Science and Engineering

journal homepage: www.elsevier.com/locate/jngse

Electromagnetic thermal stimulation of shale reservoirs for petroleum production

Jin-Hong Chen[*], Daniel T. Georgi[1], Hui-Hai Liu

[a]*Reservoir Engineering Technology, Aramco Services Company: Aramco Research Center –Houston, Texas, USA*

ABSTRACT

Light hydrocarbons produced from unconventional tight shale reservoirs with matrix permeability in nano-Darcy range accounts for more than half of the petroleum production in the United States in the past several years. This has been enabled mainly by the drilling of long horizontal wells coupled with extensive hydraulic fracturing. A typical fracturing job for a horizontal well requires two to five million gallons of water which imposes significant challenges in many areas of the world that lack water resources. In addition, treatment and disposal of produced fracturing fluids can be expensive and may negatively impact the environment. Here we show a 'water-free' stimulation method to produce light hydrocarbons from the extremely tight reservoirs using electromagnetic (EM) waves to heat the formation and elevate pore-water pressure. We demonstrated in the laboratory that microwave heating pulverized shales and other tight rocks without confinement and generated extensive fractures within shales with 15 MPa isotropic confinement pressures. Our calculation indicates that for typical shale reservoirs pore-water pressure can increase to 90 MPa or higher that is sufficient to stimulate the formation for production with a less than 100 °C temperature increase of the reservoir. Using a simplified coupled model of EM heating and thermal diffusion, we estimated that with practically reasonable amount of power input the EM heating can stimulate a sufficiently large volume of tight reservoirs to produce light hydrocarbons.

1. Introduction

Light hydrocarbons in organic-rich shales were once considered impossible to produce commercially due to the nD permeability; but now contribute approximately 50% oil and 70% gas production in 2015 in the United States (U.S.EIA, 2016a; U.S.EIA, 2016b) and are becoming globally important, having benefited from the combination of horizontal drilling and hydraulic fracturing. The estimated world recoverable light hydrocarbon reserves from shales are estimated to be 418.9 BBL oil and 7576.6 TCF gas (U.S.EIA, 2015). Approximately 4.3 million barrels oil and 53 billion cubic feet of gas per day were produced from shales alone in the U.S. (U.S.EIA, 2016a; U.S.EIA, 2016b). However, the estimated ultimate recovery (EUR) factor is small: approximately 6% for shale oil and 25% for shale gas using hydraulic fracturing (U.S.EIA, 2015). Moreover, hydraulically fracturing one well typically requires 2 to 5 million gallons of water which can be difficult to obtain in many regions in the world. In addition, reprocessing recovered fracturing water can be expensive financially and environmentally. Thus, developing water-free or water-efficient fracturing techniques is highly desirable. Here we present an alternative 'water-free' method using electromagnetic (EM) wave to heat the rock and elevate the pore-water pressure to stimulate shale reservoirs or any other tight reservoirs (Chen et al., 2015). For this paper tight reservoir are defined to have matrix permeability typical for shales, i.e., nD scale.

EM heating has long been recognized to cause differential heating of different minerals in the rocks and has been suggested for applications in energy related industries such as mineral processing, coalbed methane production, and oil-shale retorting and production. Differential heating by EM generates inhomogeneous strain in rocks and induced cracks (Cooper and Simmons, 1977). The effect was quickly recognized to be useful for rock grinding (Walkiewicz et al., 1989) and mineral separation (Kingman et al., 1998). Microwave heating is also known to pyrolyze coals (Fu and Blaustein, 1969) and to improve coal grindability (Lester et al., 2005). A recent experiment demonstrated that a short burst (3 s) of large power (15 kW) microwave induced fractures and increased cleat apertures in coal under isotropic stress (Kumar et al., 2011). EM heating has also been suggested early on to produce oil shale, tar sand, and coal (Bridges and Taflove, 1977). Specifically for oil shale, EM heating was proposed to retort kerogen into light hydrocarbon *in situ* so it can be produced. The physics behind the majority of

---

these applications includes two aspects: differences in thermal adsorption ability and thermal expansion coefficient of minerals composing the subject rock. EM may heat some components of the formation more efficiently than others and the thermal expansion coefficients can differ quite significantly (Chen et al., 2015). Consequently, fractures are generated in the rocks when the temperature increases. While all the above applications have been based on the heterogeneous mineral responses to EM heating, here we investigate the pore-water pressure increase in tight rocks due to EM heating. This is a very different mechanism than the differential heating, strain inducing mechanism; the "trapped" pore water heating and commensurate pressure elevation is a very effective mechanism to break tight rock and is a potential alternative or complementary method to stimulate shale reservoirs for production.

The method utilizes the physical fact that in a tight rock when water is heated and its volume cannot significantly change because the shale matrix permeability is in the nD range (Luffel et al., 1993) and the pore water is effectively trapped, and, thus, the pore-water pressure increase rapidly. When the pore-water pressure becomes sufficiently high, the rock fails. Consequently, formation permeability increases to more efficiently recover light hydrocarbons from these tight reservoirs.

This paper details the physics of EM heating to stimulate shale and other tight reservoirs. First we estimate the pore-water pressure elevation in a tight rock using a simplified model where the water is quickly heated and the temperature rises rapidly. We then show experimental results of microwave stimulation of tight rocks under zero confinement and under approximately 15 MPa isotropic confinements. The experimental results verify the efficacy of stimulating tight rock reservoirs with EM heating. We then estimate the power requirement for EM to stimulate a tight reservoir: we evaluate the thermal diffusion at microscale to prove that local thermal equilibrium can be readily achieved. We then calculate EM heating in macroscale and show that a reasonable amount of EM power input can raise the temperature of sufficiently large volume of a tight reservoir for EM thermal stimulation.

2. Experiments

2.1. Samples and preparation

Microwaving tests were performed on one tight Tennessee sandstone and more than 30 outcrop shale plugs from Mancos, Marcellus, and Eagle Ford. Saturation of the dry Tennessee sandstone sample was achieved by first vacuuming the plug for more than 40 h and then imbibing 2% KCl solution under vacuum condition. The shale plugs were either tested as received or placed in the solution for 5 h before the microwaving experiment. All shale plugs were cylindrical with 2.54 cm diameter and 2.54 cm length. The diameter of the Tennessee sandstone plug was 2.0 cm.

2.2. Water content determination

Water content was measured using low field NMR (2 MHz or 13 MHz) by comparing the measured NMR signal from a sample to known amount of water. The NMR signal was acquired using a CPMG spin echo method (Carr and Purcell, 1954; Meiboom and Gill, 1958).

2.3. Microwaving

Destructive microwaving tests were performed with a common household microwave (Hamilton Beach Household Microwave, Model P100N30AP_F4). The maximum microwave exposure time was set to be 45 s. The microwaving experiment was immediately terminated when the audible rock failure was detected. For experiments at zero confining pressure, samples were placed in a thick-walled glass bottle to contain the broken pieces. A small hole was drilled in the bottle cap to avoid

pressure build-up within the bottle when the sample was heated. For experiments with confinement pressure, a hole drilled in the back-wall of the microwave allowed a tube to extend outside the microwave which was connected with an external pressure regulator and valves to a high-pressure nitrogen cylinder. The sample chamber was pressurized by the nitrogen gas to provide an isotropic confinement to the tested sample. When the nitrogen gas pressure in the sample chamber reached 13.8 MPa which took less than 30 s, the valve to the pressure gas cylinder was instantly closed and the microwave was turned on to start the experiment. Microwave heating of the test sample also increased the temperature of the nitrogen gas in the chamber; as the results, the confinement pressure from the nitrogen gas increased as well. Therefore, 13.8 MPa is considered as the minimum confinement pressure the tested samples were subjected to.

2.4. In situ temperature measurement

Temperature measurement were made on samples inside an Anton Paar Manowave 300. Fiber optic sensors (FISO Technologies Inc.) were inserted into small diameter (1 mm) drilled holes in the sample. A layer of Nano Diamond Thermal Compound (Formula 7, Antec, Inc.) was painted onto the sensor to provide good thermal contact between the sensor and the rock for rapid and accurate temperature measurement. The sample was then irradiated in an Anton Paar microwave for specified time at various power levels. The fiber sensor was feed through the exhaust tube of the microwave to a computer for data logging.

3. Result

3.1. Pore-water pressure elevation with temperature increase in tight rocks

The pore-water pressure increase by heating is calculated based on a model that water is contained in the pores of nm to µm size within an impermeable rock matrix. The rock matrix is assumed to be elastically linear, as illustrated in Fig. 1a. The perturbations to the *in situ* stress field by the water-filled pores, however, are localized to within three to
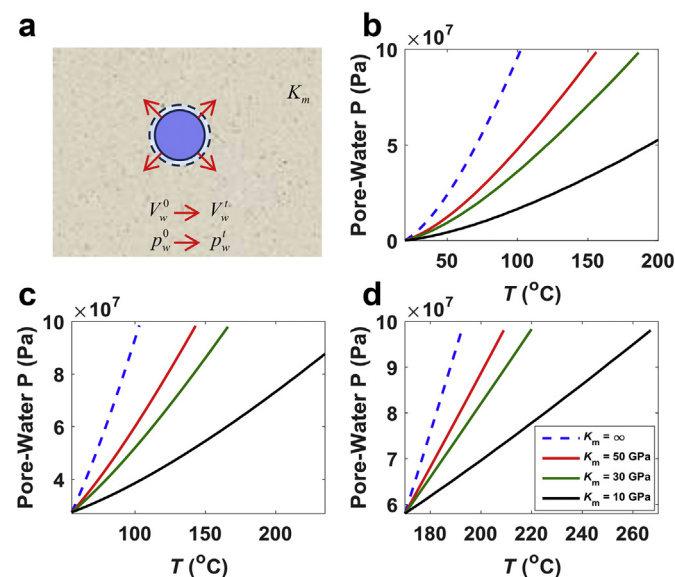

Fig. 1. Temperature dependent pore-water pressure elevation in a tight rock. **a,** illustration of a water filled pore in a rock matrix that allows the water to slightly expand when heated from the solid sphere to the dashed sphere. **b,c,d,** dependence of pore-water pressure on temperature for different rock bulk moduli at different initial conditions: **b,** $p_w^0 = 1.01 \times 10^5$ Pa, $T_w^0 = 20\,°C$, laboratory condition; **c,** $p_w^0 = 2.75 \times 10^7$ Pa, $T_w^0 = 55\,°C$, approximately corresponding to Marcellus reservoir; **d,** $p_w^0 = 5.80 \times 10^7$ Pa, $T_w^0 = 170\,°C$, approximately corresponding to Haynesville reservoir.

five radii of the pore (Jaeger et al., 2007) in μm or smaller. Therefore, change in the bulk rock volume owing to the elevation of the pore-water pressure is practically ignored. In this case, the pore-water pressure equals the stress on the rocks while the total rock volume does not change and the pore water pressure can be calculated as (Chen et al., 2015)

$$p_w = p_w^0 + \frac{K_m x_w}{(1 - x_w)}\left(\frac{V_w}{V_w^0} - 1\right) \tag{1}$$

where K_m is rock matrix bulk modulus; χ_w is the water content defined as volumetric ratio of water to the total rock; p_w and V_w are the pore-water pressure and volume, respectively, at elevated temperature T; superscript 0 in Eq. (1) refers to parameters at time 0 or initial conditions. The bulk volume water content, χ_w, and the water saturation may be very small as not all pores or pore space need be occupied by water for the process to be effective. The pore-water pressure, volume, and temperature follow an equation of state (EOS) in a tight rock where water does not flow, formally expressed as:

$$z(p_w, T_w) = \frac{p_w V_w}{RT_w} \tag{2}$$

where $R = 0.461526\,\text{kJ kg}^{-1}\cdot\text{K}^{-1}$ is the specific gas constant of ordinary water (Cooper, 2007); z is the compressibility factor and a function of pressure and temperature. We adopted a water EOS from IAPWS (Cooper, 2007; Wagner and Pruβ, 2002) which covers the temperature and pressure ranges: $0\,°\text{C} \leq T \leq 800\,°\text{C}$, $p \leq 100\,\text{MPa}$ and $800\,°\text{C} \leq T \leq 2{,}000\,°\text{C}$, $p \leq 50\,\text{MPa}$, respectively. A Matlab program was coded to calculate the pressure, temperature, and volume relationship for this water EOS (Holmgren, 2006).

The temperature dependent pore-water pressure was calculated using Eq. (1) and Eq. (2) using a bisection method (Arfken and Weber, 2013) with a Matlab program. Fig. 1b and d shows the calculated results with $\chi_w = 5\%$ and different matrix moduli K_m (legend in Fig. 1d applies for 1b and 1c, $1\,\text{GPa} = 10^9\,\text{Pa}$, $K_m = 50$, 30, and 10 GPa approximately correspond to matrix of carbonate, sandstone or shale, and kerogen, respectively) at different initial conditions: b, $p_w^0 = 1.01 \times 10^5\,\text{Pa}$, $T_w^0 = 20\,°\text{C}$, corresponding to laboratory condition; c, $p_w^0 = 2.75 \times 10^7\,\text{Pa}$, $T_w^0 = 55\,°\text{C}$, approximately corresponding to Marcellus shale (Kargbo et al., 2010); d, $p_w^0 = 5.80 \times 10^7\,\text{Pa}$, $T_w^0 = 170\,°\text{C}$, corresponding to Haynesville shales (Wang and Gale, 2009). The calculated results in Fig. 1b and c shows that the pore-water pressure elevation with increasing temperature depends on the rock matrix modulus and initial temperature and pressure conditions. For example, at laboratory condition (Fig. 1b), when temperature increases from 20 °C to 100 °C, the pore-water pressure increases more than 36 MPa ($1\,\text{MPa} = 10^6\,\text{Pa}$) when $K_m = 30\,\text{GPa}$ and only increases 17 MPa when $K_m = 10\,\text{GPa}$. At reservoir conditions, for example Fig. 1d, to raise the pore-water pressure to 90 MPa which should fail the rock using hydraulic fracturing method, only requires a temperature increase of approximately 32 °C, 48 °C, and 80 °C for rock with $K_m = 50\,\text{GPa}$, 30 GPa, and 10 GPa, respectively. For given shale reservoir, the initial reservoir temperature, pore pressure, and matrix modulus are given parameters, and, thus, the final pore-water pressure is solely dependent on the temperature increase associated with the heating.

3.2. Stimulate tight rocks using microwave heating in the laboratory

We tested the method to elevate pore-water pressure to stimulate tight rocks by increasing water temperature in the laboratory using microwaves on different tight natural and man-made rocks (Chen et al., 2015). Fig. 2 shows representative examples of tight rocks before (left column) and after (right column) microwaved for 20–35 s: a), Marcellus shale without any treatment; b), Eagle Ford shale with 5 h spontaneous water imbibition; c), tight Tennessee sandstone fully hydrated. Samples
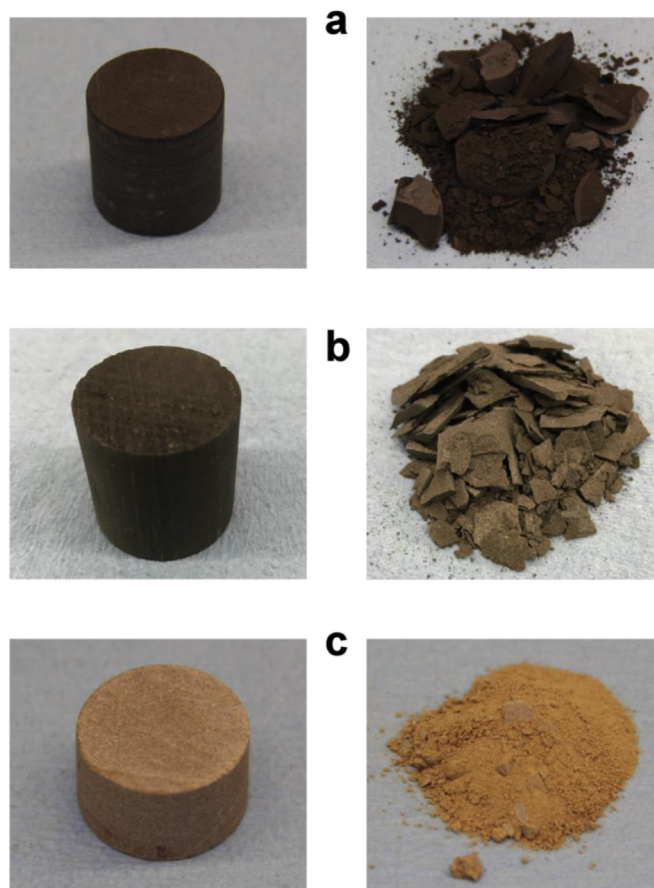

Fig. 2. Microwaving pulverizing tight rocks under zero confinement. a,b,c, are Marcellus shale, Eagle Ford shale, and tight Tennessee sandstone, respectively, before (left column) and after (right column) microwaving.

used in (a) and (b) were shale outcrops; therefore, the fluid in these samples likely is only water. We measured the water content in the samples before microwaving using low field NMR method. The measured water contents were 2.8%, 1.7%, and 6%, for samples (a), (b), and (c), respectively and the mean transverse-NMR-relaxation times were 0.7 ms, 0.4 ms, and 2.5 ms, respectively. The short relaxation time indicates the pores that hosting water are very small (Chen et al., 2012). Fig. 2 shows that the elevated pore-water pressure from microwaving heating pulverizes the tight rock samples. We have also microwaved natural tight rocks and manmade tight samples with hydrations less than 0.2% (below NMR detection limit) and have not observed any pulverization. This proved that heating induced elevation of pore-water pressure is the mechanism causing the tight rocks' failure.

We further tested the effect of elevated water-pore pressure from microwaving heating for tight rocks under isotropic confinement using a pressure holder built from microwave-transparent material (ULTEM, unreinforced polyetherimide). The parts and assembly of the pressure cell are shown in Fig. 3 from (a) to (c). Fig. 3d shows representative slices of CT images of a Mancos shale pre- and post-microwaving (two slices) as labeled under an isotropic confinement of 13.8 MPa. The process to reach the 13.8 MPa confinement pressure takes less than 30 s; therefore, any invasion of nitrogen gas into the nD-permeability rock can be neglected. Fig. 3d shows that large number of complex fractures were generated in the plugs from microwaving; however, no pulverization occurred. Fig. 3e shows slices of CT image from approximately the same location pre- and post-microwaving of a different Mancos shale plug. CT image shows that this sample has pre-existing fractures; nevertheless, microwaving generated extensive new fractures. The rings observed in some of the CT slices are artifacts from bad pixels of the X-
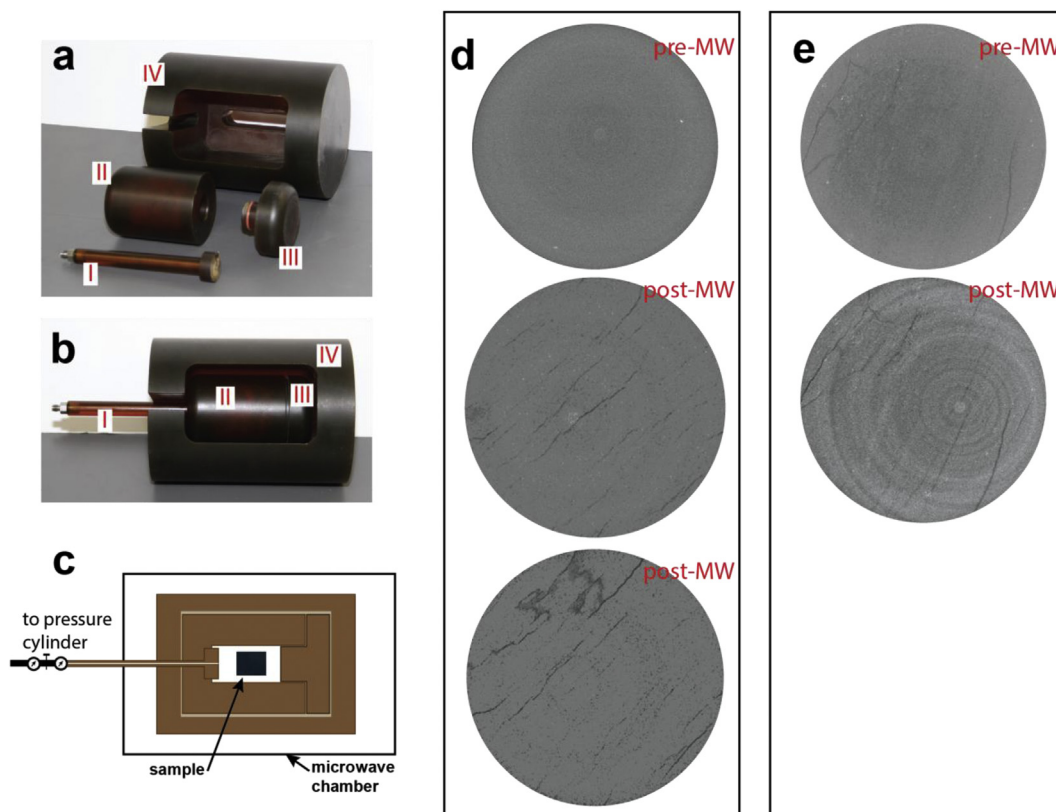
Fig. 3. | **Microwaving generates extensive fractures in shale under isotropic confinement. a,** the four parts of the pressure core holder. Part II has a chamber in the center for sample and a smaller hole at the end allowing the tube, Part I, to pass through and be connected to an external pressurized gas source. Part III is the cap to the sample chamber. Part IV holds the Part II and Part III together when the chamber is pressurized. **b**, the assembled pressure holder; **c**, illustration of the cross section of the assembled pressure holder with a sample inside the sample chamber. **d** shows representative CT image slices of a shale plug pre-microwaving and post-microwaving under minimum 13.8 MPa isotropic confinement as labeled. **e** shows CT slices approximately from the same location of a shale plug pre- and post-microwaving. Plug **e** has pre-existing fractures, in contrast to plug **d** without resolvable fracture before microwaving.

ray detector. Extensive fractures were observed in all the tested shale samples (more than 10). The extensive fractures generated by this method should allow light hydrocarbons trapped in the shale matrix to flow or diffuse to the neighboring fractures to be easily produced.

3.3. Microscale EM heating of rocks and local thermal equilibrium

We considered the heat generation by EM wave heating and local thermal redistribution in the shale reservoir rocks. The heat generated in rocks from EM waves is from two mechanisms: conductivity heating and dielectric loss heating. The average Joule heat density in a unit volume is $w = (\sigma + \omega \varepsilon'')E^2$, in which σ and ε'' are the electric

conductivity and dielectric loss of the material, respectively; ω and E are the frequency and electric field intensity of the EM wave, respectively. Table A1 in the Appendix lists the electric and thermal constants of typical components in shales and other earth formation. The last column lists the typical values found in Green River Shale. The conductivity and dielectric loss of water are several orders of magnitude larger than other major materials that form the matrix grains: quartz, calcite, and dolomite. Pyrite has EM properties similar to water. In most rocks, it is present in much smaller quantities; nevertheless, in some organic-rich shale formations pyrite concentrations can be greater than the bulk volume water. However, in most rocks, water is the major component that converts EM energy into heat. In rocks, where pyrite is
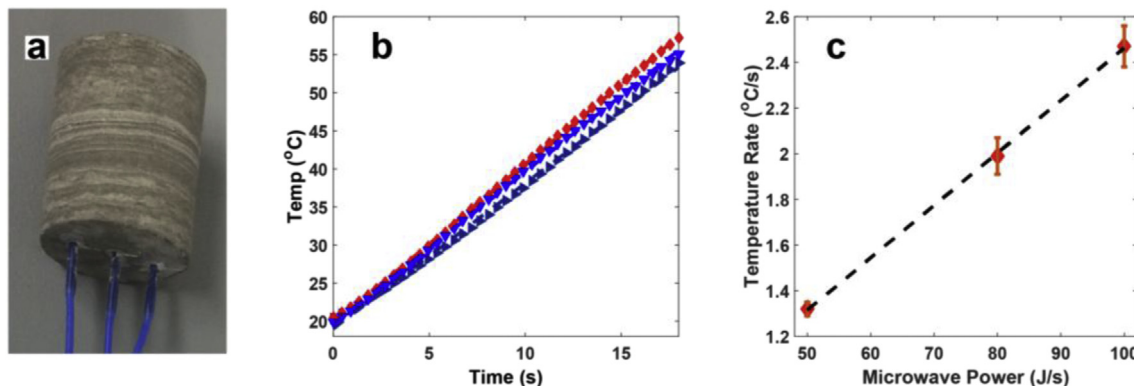

Fig. 4. In-situ temperature measurement during microwave heating. a, picture illustrating three optical cables inserted into a Mancos shale; **b,** measured temperature increase of rock subject to 80 J/s microwave radiation; **c,** plot of average temperature rate increase versus input microwave power.

present in larger volumes, it will heat rapidly and add to the heating of the formation including the trapped pore water.

Next we show that thermal diffusion results in local thermal equilibrium between pore-water and the mineral grains around the water pores. Thermal redistribution is governed by the diffusion equation (Carslaw and Jaeger, 1986); therefore, we can estimate the time, t, needed for heat with thermal diffusivity constant D_T to conduct a distance L using the Einstein diffusion relationship: $t = L^2/6D_T$ (Einstein, 1905). The thermal diffusivity $D_T = \kappa/\rho c_p$ measures the ability of a material to conduct thermal energy relative to its ability to store thermal energy, where κ is thermal conductivity, ρ is density, and c_p is the specific heat. The time needed for heat to diffuse from pore water or the grain surface to a grain center are 0.5, 1.5, and 0.8 ms for quartz, calcite, and dolomite, respectively, assuming a grain diameter of 200 μm. Typically the time for EM heating a rock is measured in seconds in the laboratory to days in reservoirs which is at least three orders of magnitude greater than the time needed to equilibrate the temperature between pore water and the neighboring grains. Therefore, local equilibrium between water and the matrix is always reached. Consequently, the thermal properties of rock under EM heating can be treated as a bulk average value although the EM interacts much more strongly with water and a few minerals. If all the input EM energy p_{in} is converted to heat, it results in a temperature increase of $\Delta T = \frac{p_{in}t}{c_p m}$, where p_{in} and m are the input EM power and the rock mass subjected to EM heating, respectively. Therefore, the temperature increase is linearly dependent on the time the rock is exposed to the EM radiation. The rate of temperature increase is proportional to the EM power: $\frac{dT}{dt} = \frac{p_{in}}{c_p m}$. These results were confirmed with the in-situ temperature measurement using fiber optic sensors in shale samples under microwaving, as shown in Fig. 4. The measurements were performed by inserting three fiber optic sensors approximately into the center of a Mancos shale (containing 3.2% water in volume) as shown in Fig. 4a. Fig. 4b shows the temperature recorded from the three sensors in the sample while it was being microwaved with a power of 80 J/s. The temperature increased linearly with time as predicted. The average temperature rate increase, dT/dt, was linearly dependent on the input microwave power, p_{in}, as predicted and is shown in Fig. 4c. The linear rate gave a constant: $\frac{1}{c_p m}$. From the fitted rate, of 0.0229 °C/J from Fig. 4c, and sample mass, 31.5 g, the specific heat for this Mancos shale, c_p, is estimated to be 1.34×10^3 J/kg/°C.

3.4. Macroscale EM thermal stimulation

We calculate in the following that EM stimulating a sufficiently large volume of a tight reservoir is possible from an energy requirement point of view. Here we ignore the heterogeneity and temperature dependence of the electrical, thermal, and mechanic properties of tight rocks. Here we still consider the tight formation does not allow significant change of water volume because although the EM heating time is much longer than in a laboratory test, the formation volume of interest here is also much larger. Some over-pressured shale reservoirs almost strictly meet the constant water volume condition. In the calculation, the reservoir is heated by irradiating the formation with EM power with an antenna in a drilled well. Accurate modeling of EM heating of the reservoir for a known antenna can be done; however, for simplicity, we assume (1) the EM is plane wave; (2) the formation is homogeneous; (3) the antenna allows the entire EM power, p_{in}, to be converted to heat in the formation. The average heat density generated by EM from the well to the formation is (detail derivation in Appendix):

$$p(r) = \frac{1}{2}(\sigma + \omega\varepsilon'')E_0^2 e^{-2k_i r}, \tag{3}$$

where E_0 is the electric field intensity at the surface of borehole, and r is the distance from the borehole surface to the formation,

$k_i = \omega\sqrt{\frac{\mu_0\varepsilon'}{2}\left[\sqrt{1 + \left(\frac{\omega\varepsilon'' + \sigma}{\omega\varepsilon'}\right)^2} - 1\right]}$ which also characterizes the penetration depth of the EM power into the formation, $\mu_0 = 4\pi \times 10^{-7}$ N/A², and ε' is dielectric constant (which together with ε'' constitutes the complex dielectric permittivity $\varepsilon = \varepsilon' + i\varepsilon''$ of the material). Ignoring end-effects, the total EM power from antenna is distributed into a cylindrical region with length L and decays radially following Eq. (3); therefore, in cylindrical coordinates $p_{in} = \int_{z=0}^{L}\int_{\theta=0}^{2\pi}\int_{r=a}^{\infty} p(r)rdrd\theta dz$ where a is the radius of the well, and the power generation rate is:

$$p(r) = \frac{2p_{in}k_i^2}{\pi L \exp(-2k_i a)(2k_i a + 1)}\exp(-2k_i r) \tag{4}$$

At the same time, the generated heat is conducted further into the formation by thermal diffusion. Considering the thermal diffusion with an EM heat source, in a cylindrical system, the temperature distribution is:

$$\frac{\partial T}{\partial t} - \frac{1}{r}\frac{\partial}{\partial r}\left(rD_T\frac{\partial T}{\partial r}\right) - \frac{2p_{in}k_i^2}{\pi L\rho c_p \exp(-2k_i a)(2k_i a + 1)}\exp(-2k_i r) = 0 \tag{5}$$

We used the following initial and boundary condition to solve Eq. (5): the stimulated region has the same initial temperature: $T(r, t = 0) = T_0$; heat transferred to and from the borehole is ignored: $\frac{\partial T(r,t)}{\partial r}\big|_{r=a} = 0$; at sufficient distance b from the borehole, the EM has zero effect to the temperature: $T(r = b, t) = T_0$. We then used the Matlab solver "pdepe" to solve Eq. (5). We used the following parameters for a shale formation: $\rho = 2.26 \times 10^3$ kg/m³ (Clark, 1966), $\kappa = 1.07$ J/S·m·K, and $c_p = 1046.7$ J/kg·K (Gilliam and Morgan, 1987), as listed in Table A1 in the Appendix. We also used the following parameters in the calculations unless specified otherwise: initial reservoir temperature, $T_0 = 170$ °C; the well radius, $a = 0.1$ m; the continuous input EM power, $p_{in} = 2 \times 10^6$ J/s; the EM irradiation time: 12 days; the antenna length and, thus, the stimulated length: $L = 100$ m; EM frequency $\omega_{EM}/2\pi = 40$ MHz; the thermal diffusivity coefficient $D_T = 1.47 \times 10^{-6}$ m²/s.

Fig. 5 shows the radial temperature distribution from the wellbore surface into the reservoir for different scenarios: **a**, the effect of thermal diffusion on temperature distribution in the reservoir; It shows that thermal diffusion efficiently redistributes heat around the wellbore. Without thermal diffusion, i.e. $D_T = 0$, 12 days EM irradiation increased the temperature at the wellbore ($r = 0$ m) to 1582 °C. Thermal diffusion reduces it to 637 °C. This is a very efficient physical phenomenon in practical applications in preventing a rapid temperature build-up at the wellbore. Furthermore, thermal diffusion transports heat further into the reservoir and, thus, can stimulate larger reservoir volume than without it. Fig. 5b is the temperature distribution with EM power input for 6, 12, and 18 days, respectively. A longer EM irradiation time generates higher temperature and also a larger stimulated reservoir volume. Fig. 5c shows the dependence of temperature distribution on the EM frequency. A dash-dotted line at 250 °C indicates the possible stimulated zone: temperatures above 250 °C can generate high pore-water pressure to stimulate the tight formation. The calculated results show that the radius of the stimulated zone is approximately 3.2 m for EM frequencies between 10 MHz and 100 MHz and reduced to 2.8 m at 400 MHz. The volume of stimulated formation is approximately 3.2×10^3 m³ using an antenna of 100 m long operating at 40 MHz and 2×10^6 J/s power for 12 days. For a typical shale gas reservoir with a 5% porosity and a local recovery rate of 75% with EM stimulation, it would produce approximately 3.63×10^4 m³ or 1.28 mmcf of gas at surface condition. For a horizontal well of 2 km long, the total stimulated zone would produce 7.26×10^5 m³ or 25.6 mmcf. Using longer stimulation time and modifying operation methods can certainly increase the stimulation volume and hence the produced total gas.
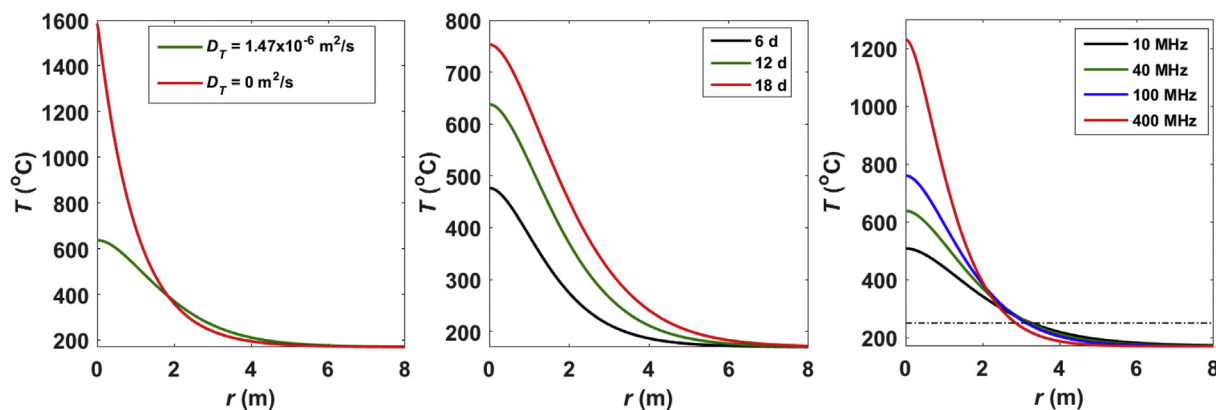
Fig. 5. Radial temperature distribution around a well for different scenarios. a, effect of thermal diffusion. **b**, effects of EM irradiation time. **c**, effect of EM frequency.

4. Discussion

This paper focused on a new mechanism of EM thermal stimulation of unconventional tight reservoirs for practical application. As we demonstrated previously, microwave heating of rocks without water was not observed to be efficient; the microwaving time was much longer than that needed to pulverize the tight rocks with water content (Chen et al., 2015). Here the experiments shown in Figs. 2 and 3 further illustrates that pore-water pressure increase from microwaving heating is a very efficient method to stimulate the tight rocks with or without confinement pressure.

The main reason that heating the pore-water generates high pressure is because in tight rocks with nD permeability, water cannot flow away and, therefore, cannot easily change its volume. As a result, the pore-water pressure elevates rapidly when its temperature increase. As demonstrated in Fig. 1 with the theoretical calculation, pore-water pressure increase faster in stiffer rocks with larger bulk modulus for the same temperature increase. For pore-waters at high pressure, their density is already high; the pressure is almost linearly dependent on the absolute temperature, as shown in Fig. 1d. This suggests that heating the pore-waters at reservoir condition would be even more efficient at elevating pore pressure than at laboratory condition which certainly would be beneficial to stimulate a tight reservoir using the EM heating.

In reference to the results shown in Fig. 2e, the Mancos shale had pre-exiting fractures prior to EM heating in some parts. Yet, microwave heating generated additional fractures; extensive fracturing was created in previously unfractured zones. This is consistent with the physical mechanism presented in this paper that the pore-water pressure elevates where water cannot expand its volume, i.e., in the tight zones. Pore-water in fractures or extremely close to fractures can easily expand its volume, and, therefore, raising the temperature does not increase pore-pressure. As a result, EM heating tends to fail the rock in the tight zones, in contrast to hydraulic fracturing which fails the rock at the 'weak' point, i.e., it is more likely open existing fractures. Therefore, EM thermal stimulation method can be applied to reservoirs that have previously been hydraulically fractured to produce the large amount of bypassed or residual hydrocarbons.

Appendix

A1 Electrical and thermal properties of common minerals in shales

Table A1

The implementation of EM thermal stimulation into deep formations will face many engineering challenges. It is worthwhile to note that downhole hardware to input millions of watts of EM power into the formation has already been built (Trauman, 2015). However, the configuration and completion of a well for production requires further study and testing and would certainly be different from what is needed for current hydraulic fracturing as practiced today. We described in a patent application an approach to optimize horizontally and vertically well spacing to maximizing production using EM thermal stimulation by drilling multiple side-wells in the tight reservoir zones (Chen et al., 2016). This method can overcome some of the disadvantage that EM heating method that only reach a few meters around the well. We also suggested in the application to take advantage of the well space to build permeability in the tight formation.

5. Conclusion

We showed that EM heating can serve as an alternative and/or supplemental simulation method for tight reservoirs to produce light hydrocarbons. The EM heating of the tight rocks elevates the pore-water pressure to break or generate complex fractures in tight reservoir rocks. Our calculation indicates that thermal diffusion plays an important role in EM heating of reservoir rocks. It leads to a fast local thermal equilibrium between formation components adsorbing EM power and the rock matrix. It also prevents rapid temperature build-up at the well-bore, critical for practical downhole implementation. We showed that with practically possible EM power input, large volumes of shale formations can be simulated for commercial production.

Acknowledgement

Electrical and thermal properties of common minerals in shales

Minerals	Brine	Quartz	Calcite	Dolomite	Pyrite	Shale
Dielectric constant ($\varepsilon_0 = 8.854 \times 10^{-12}$ F/m)	77^a	3.89 [b]	8.94 [b]	7.41 [b]	83 [c]	8 [d]
Dielectric loss ($\varepsilon_0 = 8.854 \times 10^{-12}$ F/m)	2.1×10^1 [a]	5.3×10^{-4} [b]	4.2×10^{-4} [b]	1.8×10^{-3} [b]	1.7×10^1 [c]	0.7 [d]
Resistivity ($\Omega \cdot$m)	3.6	4×10^{10} [e]	2×10^{12} [e]	$> 1.2 \times 10^3$	2.9×10^{-5} [e]	100
Thermal Conductivity (10^{-5} J/m/s/K)	0.54	6.28	2.51	5.02	37.91	1.07 [f]
Specific heat (J/kg/K)	4208	740	815	870	510	1046.7 [f]
Density (10^3 kg/m^3)	1.00	2.65	2.75	2.84	5.05	2.26
Thermal diffusivity (m^2/s)	1.29×10^{-7}	3.20×10^{-6}	1.12×10^{-6}	2.03×10^{-6}	1.47×10^{-5}	1.47×10^{-6}

All values from Clark, S. P. *Handbook of Physical Constants*. (Geological Society of America, 1966), unless specifically noted. [a] Shen, 1985; [b] Church, 1988; [c] Peng, 2014, [d] Laine, 1980; [e] Telford, 1990, [f] Gilliam.Smaller or medium values were listed when multi-values exist from the sources. Some values were deduced to fit to the frequency range (MHz) from other frequencies.

Thermal diffusivity was calculated using $K = \kappa/\rho c_p$.

a Shen, L. C. Problems In Dielectric-constant Logging And Possible Routes To Their Solution. *SPWLA* (1985).

b Church, R. H., Webb, W. E. & Salsman, J. B. Dielectric Properties of Low-Loss Minerals. *Report of Investigations 9194* (1988).

c Peng, Z., Hwang, J.-Y., Kim, B.-G., Kim, J.-Y. & Wang, X. in *Characterization of Minerals, Metals, and Materials 2014* 369–378 (John Wiley & Sons, Inc., 2014).

d Sweeney, J. J., Roberts, J. J. & Harben, P. E. Study of Dielectric Properties of Dry and Saturated Green River Oil Shale. *Energy & Fuels* **21**, 2769–2777, doi:10.1021/ef070150w (2007).

e Telford, W. M., Telford, W. M., Geldart, L. P. & Sheriff, R. E. *Applied Geophysics*. (Cambridge University Press, 1990).

f Gilliam, T. M. & Morgan, I. L. in *ORNL/TM-10499* (ed United States. DOE) (1987).

A2 Electromagnetic wave transport in lossy medium

A2.1 Electromagnetic property of the considered medium

We consider electromagnetic wave transport in a lossy medium relevant to earth materials that includes following property.

- Conductivity; however, the magnetic permeability of the medium is ignored and we have

$$\mu \approx \mu_0 \tag{A1.1}$$

$$\mu_r \approx 1 \tag{AS1.2}$$

With $\mu_0 = 4\pi \times 10^{-7}$ N/A^2; μ_r is the relative permeability.

- Dielectric loss; or the dielectric permittivity of the medium is complex as

$$\varepsilon = \varepsilon' + i\varepsilon'' \tag{A2}$$

In which ε is the complex dielectric permittivity; ε' is dielectric constant, and ε'' is dielectric loss. Note that both values are frequency ω dependent with ω the angular frequency of the EM wave. Many literature also use relative dielectric parameters as expressed

$$\varepsilon = \varepsilon_r \varepsilon_0 = \varepsilon_r' \varepsilon_0 + i\varepsilon_r'' \varepsilon_0 \tag{A3}$$

or

$$\varepsilon_r = \varepsilon_r' + i\varepsilon_r'' \tag{A4}$$

In which $\varepsilon_0 = 8.854 \times 10^{-12}$ F/m is dielectric permittivity in vacuum. ε_r' and ε_r'' are relative dielectric constant and relative dielectric loss, respectively.

A2.2 Maxwell Equations and EM wave in lossy medium

In this case, the Maxwell's Equations are

$$\nabla \cdot \mathbf{E} = 0 \tag{A5.1}$$

$$\nabla \cdot \mathbf{B} = 0 \tag{A5.2}$$

$$\nabla \times \mathbf{E} = -\frac{\partial}{\partial t}\mathbf{B} \tag{A5.3}$$

$$\nabla \times \mathbf{B} = \mu\mathbf{j} + \mu\varepsilon\frac{\partial \mathbf{E}}{\partial t} \tag{A5.4}$$

$$\mathbf{j} = \sigma\mathbf{E} \tag{A5.5}$$

E and *B* are electric and magnetic field of the EM wave, *j* is the electric density, σ is the conductivity. It may worth to note that the second term in Eq. (A5.4) on the right can be also considered as an electric density from polarization of the medium or displacement current –Maxwell term over the Ampère's Law of Eq. (A5.4).

Take the regular operation on Eq. (A5.3) and obtain

$$\nabla \times \nabla \times \mathbf{E} = -\frac{\partial}{\partial t}(\nabla \times \mathbf{B}) \tag{A5.6}$$

Using $\nabla \times \nabla \times \mathbf{E} = \nabla(\nabla \cdot \mathbf{E}) - \nabla^2 \mathbf{E}$ and inserting Eq. (A5.4) and Eq. (A5.5), Eq. (A5.6) becomes

$$\nabla^2 \mathbf{E} = \mu\varepsilon \frac{\partial^2 \mathbf{E}}{\partial t^2} + \mu\sigma \frac{\partial \mathbf{E}}{\partial t} \tag{A6.1}$$

Similarly

$$\nabla^2 \mathbf{B} = \mu\varepsilon \frac{\partial^2 \mathbf{B}}{\partial t^2} + \mu\sigma \frac{\partial \mathbf{B}}{\partial t} \tag{A6.2}$$

The solution of Eq. (A6) can be written as

$$\mathbf{E} = \mathbf{E}_0 e^{i(kr-\omega t)} \tag{A7.1}$$

$$\mathbf{B} = \mathbf{B}_0 e^{i(kr-\omega t)} \tag{A7.2}$$

where k is a complex number. Insert Eq. (A7.1) into Eq. (A6.1) we have

$$k^2 \mathbf{E} = (\mu\varepsilon\omega^2 + i\mu\sigma\omega)\mathbf{E} \tag{A8}$$

Insert Eq. (A2) to Eq. (A8), we have

$$k^2 \mathbf{E} = [\mu(\varepsilon' + i\varepsilon'')\omega^2 + i\mu\sigma\omega]\mathbf{E} \tag{A9.1}$$

or

$$k^2 = \mu\varepsilon'\omega^2 + i\mu\omega(\varepsilon''\omega + \sigma) \tag{A9.2}$$

Using complex wave vector k defined as

$$k = k_r + ik_i \tag{A10}$$

Insert Eq. (A10) into Eq. (A9.2), and we have

$$k_r^2 - k_i^2 = \mu\varepsilon'\omega^2 \tag{A11.1}$$

$$2k_r k_i = \mu\omega^2(\varepsilon'' + \sigma/\omega) \tag{A11.2}$$

Solve Eq. (A11) and we have

$$k_r = \omega \sqrt{\frac{\mu_0 \varepsilon'}{2}\left[\sqrt{1 + \left(\frac{\omega\varepsilon''\sigma}{\omega\varepsilon'}\right)^2} + 1\right]} \tag{A12}$$

$$k_i = \omega \sqrt{\frac{\mu_0 \varepsilon'}{2}\left[\sqrt{1 + \left(\frac{\omega\varepsilon''+\sigma}{\omega\varepsilon'}\right)^2} - 1\right]} \tag{A13}$$

The electric field of EM wave is then

$$\mathbf{E} = \mathbf{E}_0 e^{-k_i r} e^{i(k_r r-\omega t)} \tag{A14.1}$$

Similarly

$$\mathbf{B} = \mathbf{B}_0 e^{-\delta k_i} e^{i(k_r r-\omega t)} \tag{A14.2}$$

Therefore, the EM wave is attenuated/damped exponentially with a rate determined by k_i. The characteristic penetration depth, **skin depth δ_{sd},** is defined as E and B are attenuated to $1/e = 0.368$

$$\delta_{sd} = \frac{1}{\omega \sqrt{\frac{\mu_0 \varepsilon'}{2}\left[\sqrt{1 + \left(\frac{\omega\varepsilon''+\sigma}{\omega\varepsilon'}\right)^2} - 1\right]}} \tag{A15}$$

A2.3 Heat generation in the medium

The Joule heat generated by EM wave is

$$w = \mathbf{E}\cdot\mathbf{J} = \mathbf{E}\cdot\left(\mathbf{j} + \varepsilon\frac{\partial \mathbf{E}}{\partial t}\right) \tag{A16}$$

J is the total current density including the Maxwell term. Note that magnetic field can do no work on charged so Eq. (A16) only contains electric field. Insert Eq. (A4) and Eq. (A5.5), Eq. (A16) becomes

$$w = \mathbf{E}\cdot[\sigma\mathbf{E} - i\omega(\varepsilon' + i\varepsilon'')\mathbf{E})] \tag{A17}$$

Only the real term in Eq. (A17) generate heat so finally we have heat generated by the EM in a lossy field as

$$w = \sigma E^2 + \omega\varepsilon'' E^2 \tag{A18}$$

The first term is heat generated by conductivity and the second term by dielectric loss (the dominating microwave heating mechanism in laboratory test). Therefore the heat generated by the EM wave is

$$w = (\sigma + \omega\varepsilon'') E_0^2 e^{-2k_i r} e^{i2(k_r r-\omega t)} \tag{A19}$$

And the average heat generated by EM wave is easily evaluated from Eq. (A19) by integrating over one period of the EM wave to be

$$w = \frac{1}{2}(\sigma + \omega\varepsilon'')E_0^2 e^{-2k_i r}$$

(A20)

A3 some addition laboratory results on microwaving samples

We have microwaved shale samples from five different reservoirs, tight sandstone, pressed wet and dry clay disks, and man-made cement of various expected permeability. Fig. A1 shows some further results to illustrate water content and permeability effects on heating water to fail the rock under zero confinement pressure. Left and right columns in Fig. A1 are pre- and post-microwaving of different duration: (a) 60 s microwaving on a shale sample with water content below NMR detection and no obvious effect was observed. (b) 22 s microwaving on a cement sample with expected permeability less than 1 μD and water content of 13.4 pu. (c) 60 s microwaving on a cement sample with expected permeability of less than 1 mD and water content of 30.7 pu. The permeability for the cement samples were estimated from the materials formula. The results from (b) and (c) are in consistent with our theoretical consideration that heating can only elevate pore-water pressure in very tight samples.
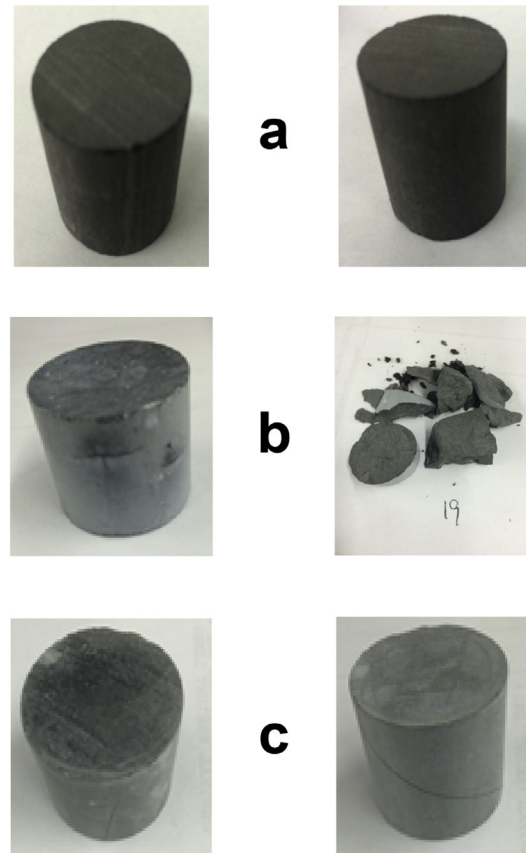

Fig. A1. Pre- and post-microwaving of different duration in left and right columns, respectively: (a) 60 s microwaving on a shale sample with water content below NMR detection. (b) 22 s microwaving on a cement sample with expected permeability less than 1 μD and water content of 13.4 pu. (c) 60 s microwaving on a cement sample with expected permeability of less than 1 mD and water content of 30.7 pu.

References

Arfken, G.B., Weber, H.J., 2013. Mathematical Methods for Physicists. Elsevier Science.

Bridges, J., Taflove, A., 1977. Apparatus and Method for in Situ Heat Processing of Hydrocarbonaceous Formations. US4144935A.

Carr, H.Y., Purcell, E.M., 1954. Effects of diffusion on free precession in nuclear magnetic resonance experiments. Phys. Rev. 94, 630–638.

Carslaw, H.S., Jaeger, J.C., 1986. Conduction of Heat in Solids. Clarendon Press.

Chen, J.-H., Zhang, J., Jin, G., Quinn, T., Frost, E., Chen, J., 2012. Capillary Condensation and NMR Relaxation Time in Unconventional Shale Hydrocarbon Resources. Society of Petrophysicists and Well-Log Analysts.

Chen, J.-H., Georgi, D., Liu, H.-H., Lai, B., 2015. Fracturing Tight Rocks by Elevated Pore-water Pressure Using Microwaving and its Applications. Society of Petrophysicists and Well-Log Analysts.

Chen, J.-H., Georgi, D.T., Liu, H.-H., Davis, L.A.J., 2016. Using Radio Waves to Fracture Rocks in a Hydrocarbon Reservoir US9896919B1.

Clark, S.P., 1966. Handbook of Physical Constants. Geological Society of America.

Cooper, J.R., 2007. Revised Release on the IAPWS Industrial Formulation 1997 for the Thermodynamic Properties of Water and Steam. Lucerne, Switzerland.

Cooper, H.W., Simmons, G., 1977. The effect of cracks on the thermal expansion of rocks. Earth Planet Sci. Lett. 36, 404–412.

Einstein, A., 1905. On the movement of small particles suspended in stationary liquids required by the molecular-kinetic theory of heat. Ann. Phys. 17, 549.

Fu, Y.C., Blaustein, B.D., 1969. Pyrolysis of coals in a microwave discharge. Ind. Eng. Chem. Process Des. Dev. 8, 257–262.

Gilliam, T.M., Morgan, I.L., 1987. Shale: measurement of thermal properties. In: U.S. DOE, ORNL/TM-10499.

Holmgren, M., 2006. X Steam, Thermodynamic Properties of Water and Steam. www.x-eng.com.

Jaeger, J.C., Cook, N.G.W., Zimmerman, R., 2007. Fundamentals of Rock Mechanics. Wiley.

Kargbo, D.M., Wilhelm, R.G., Campbell, D.J., 2010. Natural gas plays in the Marcellus shale: challenges and potential opportunities. Environ. Sci. Technol. 44, 5679–5684.

Kingman, S.W., Corfield, G.M., Rowspm, N.A., 1998. Effects of microwave radiation upon the mineralogy and magnetic processing of a massice Norwegian ilmenite ore. Magn. Electr. Separ. 9, 131–148.

Kumar, H., Lester, E., Kingman, S., Bourne, R., Avila, C., Jones, A., Robinson, J., Halleck, P.M., Mathews, J.P., 2011. Inducing fractures and increasing cleat apertures in a bituminous coal under isotropic stress via application of microwave energy. Int. J. Coal Geol. 88, 75–148.

Lester, E., Kingman, S., Dodds, C., 2005. Increased coal grindability as a result of microwave pretreatment at economic energy inputs. Fuel 84, 423–427.

Luffel, D.L., Hopkins, C.W., Schettler, P.D.J., 1993. Matrix Permeability Measurement of

Gas Productive Shales. Society of Petroleum Engineers, pp. 261–270.

Meiboom, S., Gill, D., 1958. Modified spin-echo method for measuring nuclear relaxation times. Rev. Sci. Instrum. 29, 688–691.

Trauman, M., 2015. Personal Communication.

U.S.EIA, 2015. Table: world shale resource Assessments. Retrieved from. https://www.eia.gov/analysis/studies/worldshalegas/.

U.S.EIA, 2016a. Hydraulic Fracturing Accounts for about Half of Current U.S. Crude Oil Production. http://www.eia.gov/todayinenergy/detail.cfm?id = 25372.

U.S.EIA, 2016b. Hydraulically Fractured Wells Provide Two-thirds of U.S. Natural Gas

Production. http://www.eia.gov/todayinenergy/detail.cfm?id = 26112.

Wagner, W., Pruß, A., 2002. The IAPWS formulation 1995 for the thermodynamic properties of ordinary water substance for general and scientific use. J. Phys. Chem. Ref. Data 31, 387–535.

Walkiewicz, J.W., Raddatz, A.E., McGill, S.L., 1989. Microwave-assisted grinding. In: Industry Applications Society Annual Meeting, Conference Record of the 1989, vol. 1522. IEEE, pp. 1528–1532 1989.

Wang, F.P., Gale, J.F.W., 2009. Screening criteria for shale-gas systems. Gulf Coast Association of Geological Societies Transactions 59, 779–793.